Oxysterol-binding protein homologs mediate sterol transport from the endoplasmic reticulum to mitochondria in yeast

Received for publication, October 24, 2017, and in revised form, February 9, 2018 Published, Papers in Press, February 27, 2018, DOI 10.1074/jbc.RA117.000596

Siqi Tian[‡1], **Akinori Ohta**[§], **Hiroyuki Horiuchi**[‡], **and Ryouichi Fukuda**[‡2]

From the [‡]*Department of Biotechnology, The University of Tokyo, Yayoi 1-1-1, Bunkyo-ku, Tokyo 113-8657, Japan and* [§]*Department of Biological Chemistry, College of Bioscience and Biotechnology, Chubu University, 1200 Matsumoto-cho, Kasugai, Aichi 487-8501, Japan*

Edited by Dennis R. Voelker

Sterols are present in eukaryotic membranes and significantly affect membrane fluidity, permeability, and microdomain formation. They are synthesized in the endoplasmic reticulum (ER) and transported to other organelles and the plasma membrane. Sterols play important roles in the biogenesis and maintenance of mitochondrial membranes. However, the mechanisms underlying ER-to-mitochondrion sterol transport remain to be identified. Here, using purified yeast membrane fractions enriched in ER and mitochondria, we show that the oxysterol-binding protein homologs encoded by the *OSH* genes in the yeast *Saccharomyces cerevisiae* mediate sterol transport from the ER to mitochondria. Combined depletion of all seven Osh proteins impaired sterol transport from the ER to mitochondria *in vitro*; however, sterol transport was recovered at different levels upon adding one of the Osh proteins. Of note, the sterol content in the mitochondrial fraction was significantly decreased *in vivo* after Osh4 inactivation in a genetic background in which all the other *OSH* genes were deleted. We also found that Osh5–Osh7 bind cholesterol *in vitro*. We propose a model in which Osh proteins share a common function to transport sterols between membranes, with varying contributions by these proteins, depending on the target membranes. In summary, we have developed an *in vitro* system to examine intracellular sterol transport and provide evidence for involvement of Osh proteins in sterol transport from the ER to mitochondria in yeast.

Sterols are found in the eukaryotic organellar membranes and plasma membrane at distinct concentrations and have significant effects on membrane fluidity, permeability, and microdomain formation (1, 2). They are either *de novo* synthesized in the endoplasmic reticulum (ER)[3] or taken up from outside the cells, making intermembrane sterol transport critical for membrane homeostasis by the maintenance of membrane sterol levels (3). Intermembrane sterol transport is considered to be carried out by vesicular and nonvesicular mechanisms. Nonvesicular sterol transport (4–7) has been proposed to be mediated by lipid transfer proteins and/or through membrane contact sites; however, the mechanism remains elusive (8). Oxysterol-binding protein (OSBP)-related proteins (ORPs), including OSBP homologs (Osh1–Osh7) of *Saccharomyces cerevisiae*, are candidates for lipid transfer proteins that transport sterols (9). Mammalian OSBP, ORP9, and the OSBP-related domain (ORD) of ORP5, as well as yeast Osh4 have been shown to transport sterols between liposomes *in vitro* (10–12). In contrast, yeast Osh6 and Osh7 and mammalian ORP5 and ORP8 have been reported to transport phosphatidylserine (PS) from the ER to plasma membrane (13, 14). In addition, roles of ORPs as lipid sensors or regulatory proteins in various cellular processes have also been proposed (9). Therefore, the precise molecular functions of ORPs are still debated. In *S. cerevisiae*, none of the seven *OSH* genes are essential for cell viability; however, their combined deletion cause lethality, indicating a shared and overlapping essential function (15), which is yet undetermined.

Sterols play important roles in the biogenesis and maintenance of mitochondrial membranes (16, 17), and the synthesis of ergosterol, a yeast major sterol, is crucial for mitochondrial morphogenesis in *S. cerevisiae* (18). In mammals, cholesterol is transported to mitochondria and used for the synthesis of steroid hormones, oxysterols, and hepatic bile acids (17, 19). However, the molecular mechanisms underlying sterol transport from the ER to mitochondria remain unclear. In this study, we constructed a system to evaluate sterol transport from the ER to mitochondria *in vitro* using membrane fractions from yeast and analyzed the molecular mechanism. Our results suggest that Osh proteins mediate sterol transport from the ER to mitochondria.

Results

In vitro sterol transport from the ER to mitochondria

We have previously constructed a system to analyze sterol transport from the ER to mitochondria *in vivo* in *S. cerevisiae* (20). In this system, sterol transport was evaluated by measuring the content of steryl ester synthesized by a mitochondrially

This work was supported in part by Japan Society for the Promotion of Science KAKENHI Grants 17688005, 20580072, and 16J00457; a grant from Asahi Group Foundation; and a grant from the Public Foundation of Elizabeth Arnold-Fuji. The authors declare that they have no conflicts of interest with the contents of this article.

[1] A Research Fellow of the Japan Society for Promotion of Science.

[2] To whom correspondence should be addressed. Tel.: 81-3-5841-5178; Fax: 81-3-5841-8015; E-mail: afukuda@mail.ecc.u-tokyo.ac.jp.

[3] The abbreviations used are: ER, endoplasmic reticulum; EGFP, enhanced green fluorescent protein; OSBP, oxysterol-binding protein; ORD, OSBP-related domain; ORP, OSBP-related protein; PI4P, phosphatidylinositol 4-phosphate; PS, phosphatidylserine; StART, steroidogenic acute regulatory protein-related lipid transfer; mito, mitochondrial.

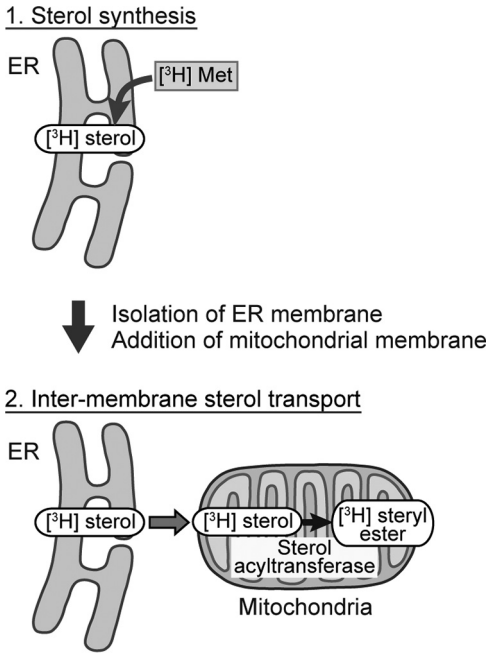

Figure 1. A scheme to measure transport of sterol synthesized in the ER to mitochondria.

targeted recombinant sterol acyltransferase, SatA, from *Aeromonas salmonicida* (mito-SatA-EGFP) in a yeast mutant deleted for *ARE1* and *ARE2* encoding acyl-CoA:sterol acyltransferases (*are1*Δ*are2*Δ). SatA is a homolog of glycerophospholipid:cholesterol acyltransferases, and it is thus considered to use phospholipids as acyl donors (21). Here, to elucidate the mechanism of the transport of sterol synthesized in the ER to mitochondria, we constructed a system to evaluate the sterol transport *in vitro* using isolated yeast organelle membranes (Fig. 1). In this system, ^{3}H-labeled sterol was first synthesized in the donor ER membrane prepared from the *are1*Δ*are2*Δ strain (22). The ER membrane was recovered and subsequently incubated with the mitochondrial membrane prepared from the *are1*Δ*are2*Δ strain expressing mito-SatA-EGFP (20). If the ^{3}H-labeled sterol is transported from the ER to mitochondria, it is predicted to be esterified by mito-SatA-EGFP.

In *S. cerevisiae*, the mitochondria are fully developed in medium containing nonfermentable carbon sources, and we used the mitochondrial fraction prepared from the *are1*Δ*are2*Δ strain expressing mito-SatA-EGFP cultured in medium containing lactate for *in vitro* sterol transport reaction. A significant amount of steryl ester was detected in the mitochondrial fraction of the *are1*Δ*are2*Δ strain expressing mito-SatA-EGFP, suggesting that mito-SatA-EGFP is active in mitochondria (Fig. 2*A*). The ER and cytosolic fractions were prepared from the *are1*Δ*are2*Δ strain cultured in medium containing glucose (Fig. 2*B*).

When the ER fraction containing ^{3}H-labeled sterol was incubated with the mitochondria and cytosolic fractions, ^{3}H-labeled sterol was esterified to steryl ester in a time-dependent manner (Fig. 2*B*), suggesting that sterol synthesized in the ER was transported to the mitochondria *in vitro*. Sterol esterification was also observed in the absence of the cytosolic fraction, but its efficiency was slightly lower than that in its presence. Sterol esterification in the absence of cytosol could be in part due to sterol transport mediated by Osh proteins associated with membranes (see below). Addition of ATP, EDTA, or divalent cations to the reaction did not show significant effect on the sterol esterification (Fig. 2, *C* and *D*). The mitochondrial membrane appeared to be intact after the reaction because Cox2 was resistant to proteinase K treatment (Fig. 2*E*).

Sterol transport from the ER to mitochondria mediated by Osh4

We next investigated the involvement of Osh proteins in sterol transport from the ER to mitochondria. Osh1–Osh3, Osh6, and Osh7 were reported to localize to the ER (23, 24). In addition, although Osh4 was known to localize in the cytosol and to Golgi (25), significant amounts of Osh4 tagged with 3×FLAG (Osh4-FLAG) expressed at physiological level, confirmed to be functional (Fig. 3*A*), were recovered in the ER-enriched fraction (Fig. 3*B*). Trace amounts of Osh4-FLAG were found in the mitochondrially enriched fraction, which could be due to the contamination by ER or other membranes. In contrast, a cytosolic marker, Pgk1, was exclusively recovered in the cytosolic fraction (Fig. 3*B*).

To exclude the effect of Osh proteins associated with membranes, sterol transport was examined using membrane and cytosolic fractions prepared from the strains having genetic backgrounds that bear the wildtype (WT) *OSH4* or the temperature-sensitive allele *osh4-1* along with the deletions of the other six *OSH* genes (*osh*Δ *OSH4* and *osh*Δ *osh4-1*) (26) (Fig. 4*A*). First, sterol was synthesized *in vitro* using the ER fractions at permissive temperature (25 °C). Similar amounts of ^{3}H-labeled sterol were obtained in the ER fractions from both strains (Fig. 4*B*). The ER fractions with ^{3}H-labeled sterol were then incubated with the mitochondrial fractions from the same background strains expressing mito-SatA-EGFP in the presence of the cytosolic fractions at nonpermissive temperature (37 °C) (Fig. 4*C*). The conversion of sterol to steryl ester was found to be lower in the reaction using the fractions from the *osh*Δ *osh4-1* strain compared with that using the fractions from the *osh*Δ *OSH4* strain. Next, the effect of Osh4 inactivation was examined using the cytosolic fraction of the WT, *osh*Δ *OSH4*, or *osh*Δ *osh4-1* strain with the ER and mitochondrial fractions of the *osh*Δ *osh4-1* strain. The ER with cytosolic fractions and the mitochondrial fraction were separately preincubated at 25 or 37 °C for 30 min after which these fractions were mixed and incubated for 1 h (Fig. 4*D*). At 25 °C, lower sterol esterification was observed in the presence or absence of the cytosolic fraction of *osh*Δ *OSH4* or *osh*Δ *osh4-1* strain compared with that in the presence of the cytosolic fraction of the WT strain. At 37 °C, sterol esterification was similarly lower in the presence of the *osh*Δ *OSH4* cytosolic fraction than in the presence of the WT cytosolic fraction. In addition, the sterol esterification was significantly lower in the reaction containing the *osh*Δ *osh4-1* cytosolic fraction than that with the *osh*Δ *OSH4* cytosolic fraction. These results suggest the involvement of *OSH* genes in the transport of sterol *in vitro*. Inactivation of Osh4 did not affect the enzymatic activity of mito-SatA-EGFP (Fig. 4*E*). To further verify the sterol transport function of Osh4, bacterially

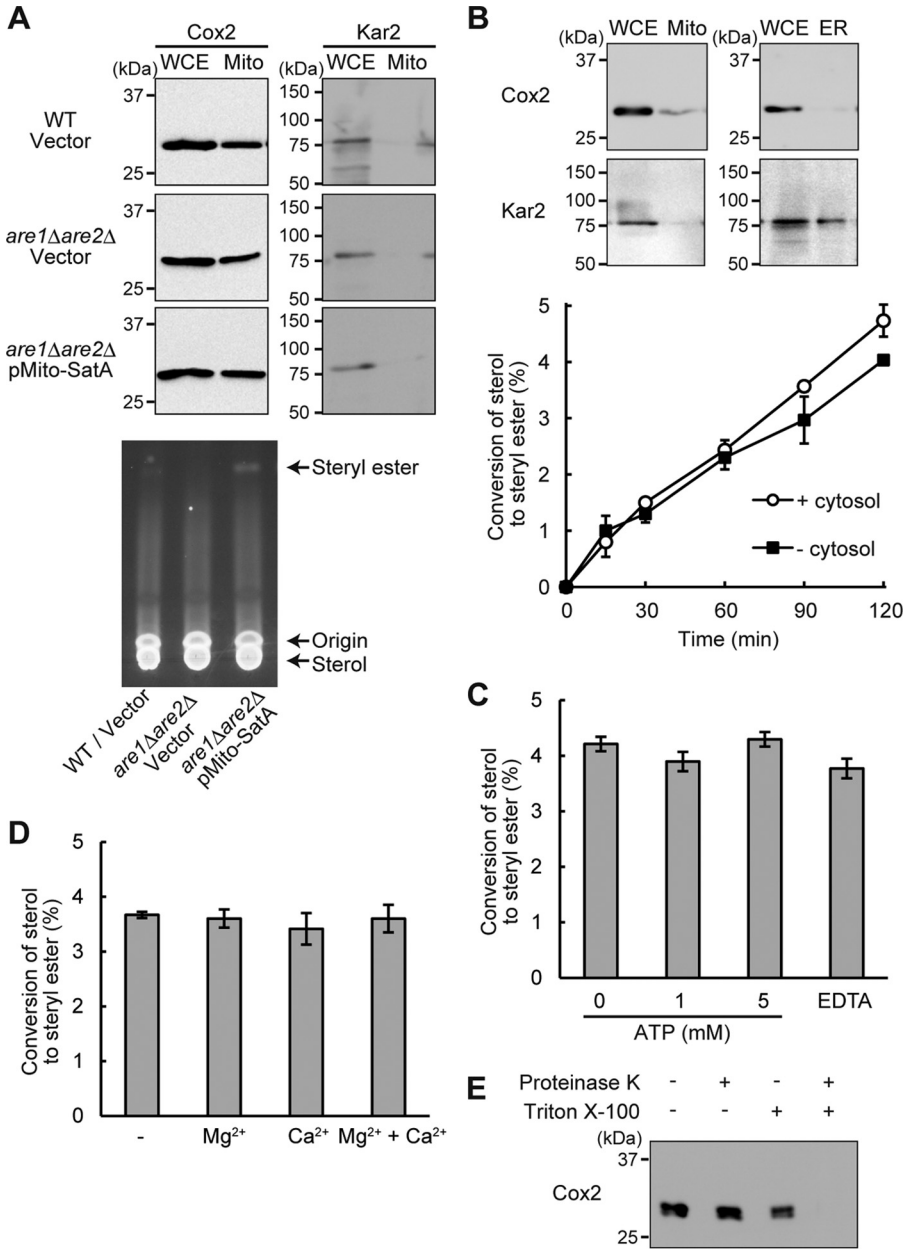

Figure 2. *In vitro* sterol transport with the ER and mitochondrial fractions from the WT strain. *A*, accumulation of steryl ester in the mitochondrial fraction of the *are1*Δ*are2*Δ strain expressing mito-SatA-EGFP. *Upper panel*, preparation of the mitochondrial fractions from the WT strain and *are1*Δ*are2*Δ strain harboring pMito-SatA or YCplac33. Recovery of the mitochondrial fractions was confirmed by Western blotting using antibodies against the ER marker Kar2 and the mitochondria marker Cox2. *Lower panel*, analysis of sterol and steryl ester in the mitochondrial fractions. Lipids were extracted and separated by TLC, and sterols and steryl esters were analyzed. *B*, *in vitro* sterol transport. *Upper panel*, preparation of the ER and mitochondrial fractions from the *are1*Δ*are2*Δ strains. Recovery of the ER and mitochondrial fractions was confirmed by Western blotting using antibodies against Kar2 and Cox2. *Lower panel*, the ER fraction from the *are1*Δ*are2*Δ strain and the mitochondrial fraction from the *are1*Δ*are2*Δ strain expressing mito-SatA-EGFP were incubated in the presence or absence of the cytosolic fractions from the *are1*Δ*are2*Δ strain at 30 °C. Data are the mean of three independent experiments. *Error bars* represent S.E. *C*, requirement of ATP for *in vitro* sterol transport. Sterol transport was measured *in vitro* using the fractions of the *are1*Δ*are2*Δ strain in the presence or absence of 1 or 5 mM ATP or 5 mM EDTA at 30 °C for 1 h. Data are the mean of triplicates. *Error bars* represent S.E. *D*, requirement of divalent cations for *in vitro* sterol transport. Sterol transport was measured *in vitro* using the fractions of the *are1*Δ*are2*Δ strain in the presence or absence of 5 mM Mg^{2+} and/or Ca^{2+} at 30 °C for 1 h. Data are the mean of triplicates. *Error bars* represent S.E. *E*, integrity of the mitochondrial membranes during the *in vitro* sterol transport reaction. After the sterol transport reaction, samples were treated with proteinase K in the absence or presence of 0.2% Triton X-100. Cox2 was detected by Western blotting using antibody against Cox2. *WCE*, whole-cell extract.

expressed and purified His_6-tagged Osh4 (His_6-Osh4) (Fig. 5*A*) was added to the transport reaction having the membrane fractions from the *osh*Δ *osh4-1* strain at 37 °C. The amount of Osh4 added to the reaction was calculated according to the reported numbers of Osh4 molecules per cell (27). Although the effect of addition of an equivalent amount of His_6-Osh4 to the cytosolic fraction was less significant, the addition of 10–50 times more Osh4 facilitated the sterol esterification (Fig. 5*B*), suggesting that sterol transport from the ER to mitochondria is mediated by Osh4. It has been shown that methyl-β-cyclodextrin can transfer cholesterol between liposomes (28). Methyl-β-cyclodextrin was suggested to transfer sterol from the ER to mito-

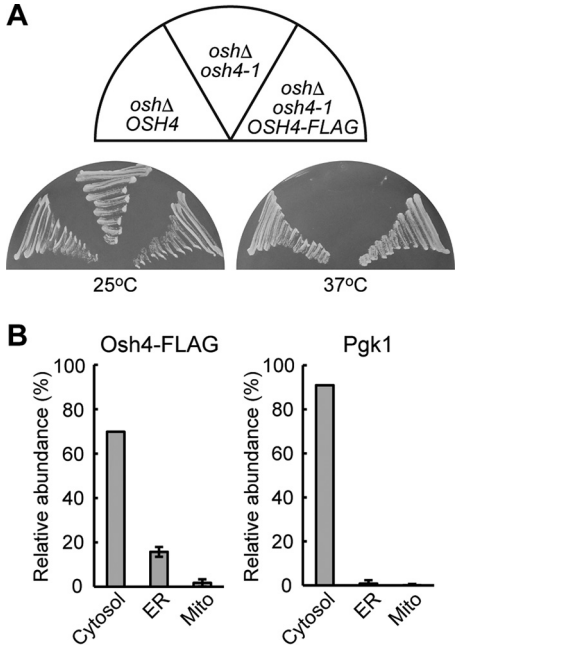

Figure 3. Subcellular distribution of Osh4. *A*, growth of the *oshΔ osh4-1* strain expressing Osh4-FLAG. The *oshΔ OSH4*, *oshΔ osh4-1*, and *oshΔ osh4-1* strains expressing Osh4-FLAG were cultured on SD medium at 25 or 37 °C. *B*, subcellular distribution of Osh4. The relative amount of each protein recovered in the fraction relative to that in the whole-cell extract is shown. Data are the mean of three independent experiments. *Error bars* represent S.E.

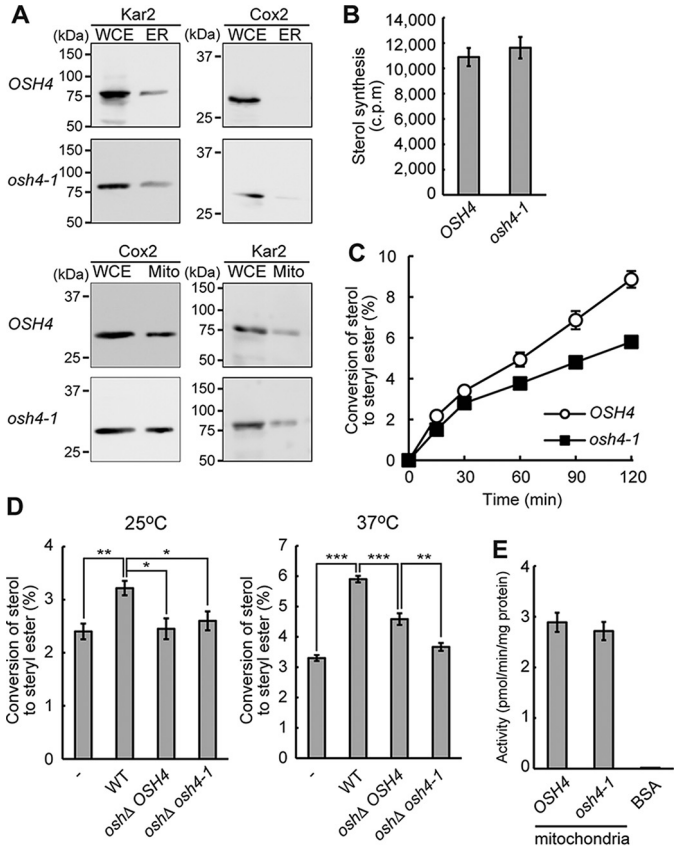

Figure 4. Involvement of *OSH4* in the sterol transport from the ER to mitochondria *in vitro*. *A*, preparation of the ER and mitochondrial fractions from the *oshΔ OSH4* and *oshΔ osh4-1* strains. Recovery of the ER and mitochondrial fractions was confirmed by Western blotting using anti-Kar2 and anti-Cox2 antibodies. *B*, sterol synthesis *in vitro*. Sterols were synthesized using the ER fractions of the *oshΔ OSH4* and *oshΔ osh4-1* strains at 25 °C for 1 h. Data are the mean of three independent experiments. *Error bars* represent S.E. *C*, *in vitro* sterol transport using the ER, mitochondrial, and cytosolic fractions of the *OSH* mutant strains. The fractions from the *oshΔ OSH4* strain (*OSH4*) and *oshΔ osh4-1* strain (*osh4-1*) were mixed and incubated at 37 °C. Data are the mean of three independent experiments. *Error bars* represent S.E. *D*, *in vitro* sterol transport using the ER and mitochondrial fractions from the *oshΔ osh4-1* strain with the cytosolic fraction of the WT, *oshΔ OSH4*, or *oshΔ osh4-1* strain. All fractions were preincubated at 25 or 37 °C for 30 min after which they were mixed and incubated at the same temperature for 1 h. Data are the mean of triplicates of two independent experiments. *Error bars* represent S.E. *, $p < 0.05$; **, $p < 0.01$; ***, $p < 0.001$ (unpaired *t* test, two-tailed). *E*, sterol acyltransferase activities of the mitochondrial fractions of the *oshΔ OSH4* and *oshΔ osh4-1* strains. Sterol acyltransferase activities in the mitochondrial fractions from the *oshΔ OSH4* and *oshΔ osh4-1* strains were measured at 37 °C. Data are the mean of triplicates. *Error bars* represent S.E. *WCE*, whole-cell extract.

chondria in our *in vitro* system more efficiently than Osh4 (Fig. 5*C*).

Involvement of Osh4 in the maintenance of mitochondrial sterol level

We next examined the sterol transport *in vivo* in the *OSH* mutants expressing mito-SatA-EGFP as described previously (20). Although similar amounts of sterol were synthesized in these strains at 25 °C, sterol synthesis was extremely lower in the *oshΔ osh4-1* strain compared with the *oshΔ OSH4* strain at 37 °C (Fig. 6*A*), and accurate evaluation of the sterol transport was difficult. Therefore, the ER and mitochondrial fractions were prepared from the *oshΔ OSH4* and the *oshΔ osh4-1* strains cultured at permissive or nonpermissive temperature (Fig. 6*B*), and their levels of ergosterol were quantified (Fig. 6*B*). Sterol contents normalized by the amounts of phosphorus derived from phospholipids in the whole-cell extracts, ER-enriched fractions, and mitochondrially enriched fractions were similar between the *oshΔ OSH4* and *oshΔ osh4-1* strains cultured at 25 °C. In contrast, the sterol content in the mitochondrial fraction of the *oshΔ osh4-1* strain cultured at 37 °C was significantly lower than that of the *oshΔ OSH4* strain cultured under the same condition, whereas that in the ER fraction of the *oshΔ osh4-1* was similar to that of the *oshΔ OSH4* strain. These *in vivo* results indicate the involvement of *OSH4* in the maintenance of sterol content in the mitochondria. The sterol content of the whole-cell extract was lower in the *oshΔ osh4-1* strain cultured at 37 °C than in the *oshΔ OSH4* strain in agreement with the decreased sterol synthesis in the *oshΔ osh4-1* strain at 37 °C (Fig. 6*A*). Sterol synthesis may be inhibited in the *oshΔ osh4-1* strain at 37 °C due to the defect in the sterol export from the ER to other membranes (see below). The mitochondrial protein Cox2 was detected in the ER-enriched fractions from the *oshΔ osh4-1* strain, but not much Cox2 was detected in those from the *oshΔ OSH4* strain. The temperature-sensitive mutation of *osh4-1* might affect separation of the ER and mitochondria.

Transport of sterol mediated by other Osh proteins

Furthermore, we examined whether other Osh proteins have the ability to transport sterol. The addition of Osh5, Osh6, and Osh7 to the *in vitro* sterol transport reaction having the membrane fractions from the *oshΔ osh4-1* strain at 37 °C elevated the sterol esterification to higher levels than did addition of Osh4 (Figs. 5*A* and 7*A*). Using GC-MS, it was determined that

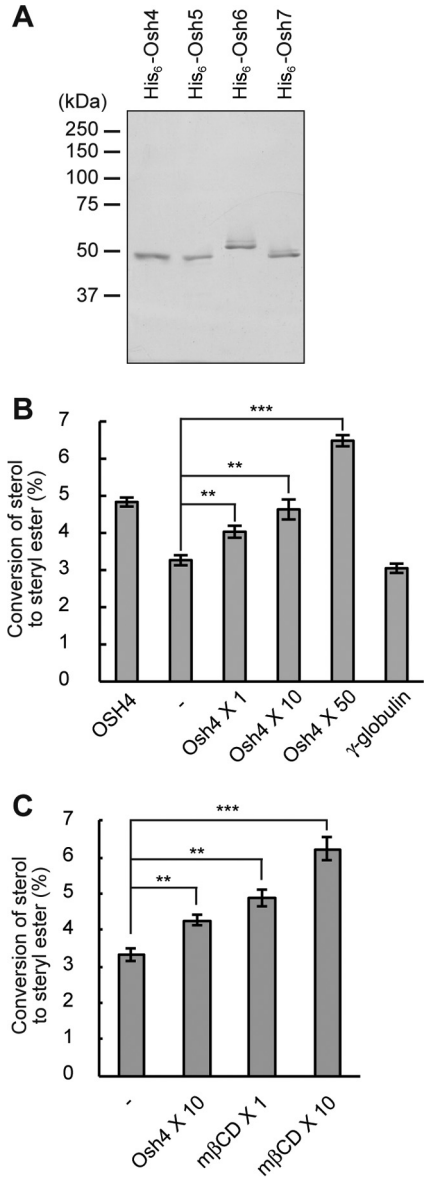

Figure 5. Sterol transport mediated by Osh4 from the ER to mitochondria *in vitro*. *A*, purification of His_6-tagged Osh proteins. His_6-tagged proteins were expressed in *E. coli* and purified. The purity of each protein was confirmed by Coomassie Blue staining. *B*, *in vitro* sterol transport using recombinant His_6-Osh4 protein. Sterol transport was measured *in vitro* using the ER and mitochondrial fractions from the *oshΔ osh4-1* strain in the presence or absence of 200 μg of the cytosolic fraction of the *oshΔ OSH4* (*oshΔ OSH4* cytosol); 5.2, 52, or 260 pmol of His_6-Osh4 (*Osh4* × *1*, × *10*, or × *50*, respectively); or 12.9 μg of γ-globulin (same weight as 260 pmol of His_6-Osh4) at 37 °C after preincubation at 37 °C for 30 min. Data are the mean of triplicates of two independent experiments. *Error bars* represent S.E. **, $p < 0.01$; ***, $p < 0.001$ (unpaired *t* test, two-tailed). *C*, *in vitro* sterol transport using methyl-β-cyclodextrin. Sterol transport was measured *in vitro* using the ER and mitochondrial fractions from the *oshΔ osh4-1* strain in the presence or absence of 52 pmol (× *10*) His_6-Osh4 or 5.2 or 52 pmol of methyl-β-cyclodextrin (*mβCD*) (× *1* or × *10*, respectively) at 37 °C for 1 h after 30-min preincubation. Lipids were extracted and counted. Data are the mean of the four experiments. *Error bars* represent S.E. **, $p < 0.01$; ***, $p < 0.001$ (unpaired *t* test, two-tailed).

4.0 nmol of ergosterol/reaction was included in the ER fraction used in the *in vitro* sterol transport assay. Thus, rates of sterol transport by these Osh proteins are calculated to be 0.092, 0.18, 0.17, and 0.15 ergosterol molecules/Osh protein/min for Osh4, Osh5, Osh6, and Osh7, respectively. Although Osh6 and Osh7 were reported to transport PS from the ER to plasma mem-

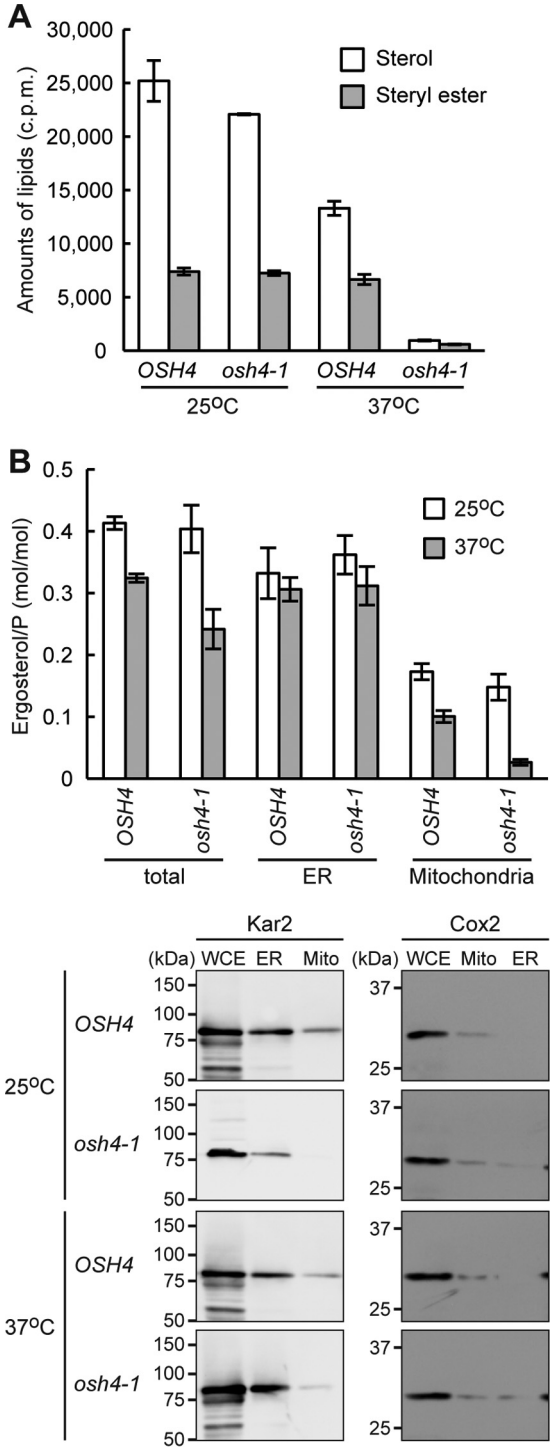

Figure 6. Role of Osh4 in the maintenance of mitochondrial sterol level *in vivo*. *A*, sterol synthesis and transport in the mutant strains defective in *OSH* genes. The *oshΔ OSH4* and *oshΔ osh4-1* strains expressing mito-SatA-EGFP were preincubated at 25 or 37 °C for 30 min and labeled with L-[*methyl*-^{3}H]methionine for 5 min. Radioactivities in sterols (*white bars*) and steryl esters (*gray bars*) were determined. Data are the mean of three independent experiments. *Error bars* represent S.E. *B*, sterol contents in the ER and mitochondrial fractions of the mutant strains defective in *OSH* genes. *Upper panel*, the *oshΔ OSH4* and *oshΔ osh4-1* strains were incubated at 25 (*white bars*) or 37 °C (*gray bars*) for 80 min. Data are the mean of three independent experiments. *Error bars* represent S.E. *Lower panel*, recovery of the ER and mitochondrial fractions from the *oshΔ OSH4* and *oshΔ osh4-1* strains cultured at 25 or 37 °C was confirmed by Western blotting using anti-Kar2 and anti-Cox2 antibodies. Similar results were obtained in three independent experiments. *WCE*, whole-cell extract. *Ergosterol/P*, ergosterol/phosphorus.

brane (13), the results of our sterol binding assay indicate that Osh6, Osh7, and Osh5 bind to sterol with significant affinities (Fig. 7*B*). The K_d values of Osh4, Osh5, Osh6, and Osh7 are 270 ± 40, 920 ± 370, 820 ± 290, and 850 ± 330 nM, and their B_{max} values are 4.1 ± 0.3, 17 ± 5, 16 ± 4, and 16 ± 5 mM, respectively. Because Osh1–Osh3 proteins could not be purified using the bacterial expression system, we used the cytosolic fraction of the yeast strain that has *OSH1*, *OSH2*, or *OSH3* expressed under the native promoter with deletions of the other *OSH* genes. The addition of these cytosolic fractions was found to elevate the sterol esterification in the sterol transport reaction (Fig. 7*C*), suggesting that Osh1–Osh3 proteins also have the ability to mediate transport of sterol. Because the numbers of Osh1 and Osh2 molecules in the cell were reported to be much lower than that of Osh4 (27), they may be able to transport sterol more efficiently than Osh4. It was reported that the number of Osh3 molecules per cell was not significantly different from that of Osh1 (27), and lower sterol transport activity of Osh3 could be due to its lower affinity to sterol molecules (29).

Discussion

Because sterols are synthesized in the ER, intermembrane sterol transport is critical for maintaining sterol contents in other organelles and the plasma membrane. Mitochondria are independent of vesicle transport and thus provide an excellent model to study nonvesicular sterol transport. Here, we established a system to evaluate sterol transport from the ER to mitochondria using yeast membrane fractions *in vitro* and analyzed the mechanism. Our results suggest that Osh proteins are involved in sterol transport from the ER to mitochondria. Because Osh4–Osh7 bound cholesterol *in vitro* (Fig. 7*B*), it is possible that Osh proteins directly transport sterol from the ER to mitochondria.

ORPs are widely conserved in eukaryotes, and multiple paralogs of ORP genes are encoded in their genomes. It has been suggested that *OSH* genes of *S. cerevisiae* share an overlapping essential function (15). Although it has been shown that a subset of ORPs in mammals and yeast transport sterols between liposomes *in vitro* (10–12), yeast Osh6 and Osh7 and mammalian ORP5 and ORP8 have been reported to mediate transport of PS from the ER to plasma membrane (13, 14). It was reported that Osh6, Osh7, and ORP5 do not bind to sterols (13). However, Osh6 and Osh7 were suggested to transport cholesterol between liposomes *in vitro*, albeit more slowly than Osh4 and Osh5 (23). In addition, ORP5 and ORP8 were suggested to bind or transport sterols *in vitro* (12, 30). Therefore, it is plausible that Osh6 and Osh7 transport sterols between biological membranes. The possibility that binding to phosphatidylinositol 4-phosphate (PI4P) could be a unifying feature of all ORPs and that only a subset of ORP family members also bind sterols has been proposed (9). Furthermore, ORPs have been proposed to function as lipid sensors or regulators in exocytosis (31), plasma membrane sterol organization (32), ceramide transport (33, 34), phosphoinositide metabolism (35), TORC1 signaling and nitrogen sensing (36), phospholipid synthesis (37), extracellular signal–regulated kinase (ERK) signaling (38), STAT3 signaling (39), and regulation of the ABC transporter (40). Therefore, common molecular functions of ORPs have remained unclear.

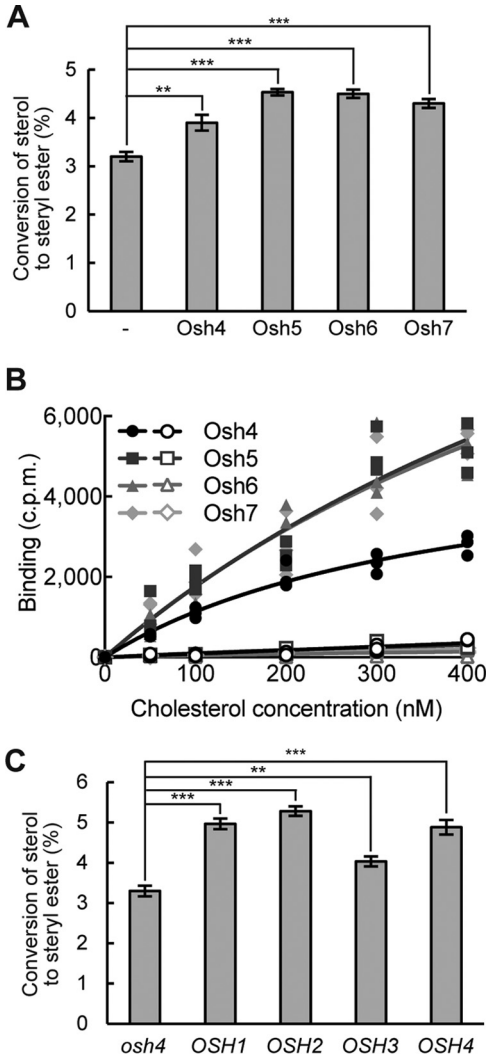

Figure 7. Transport of sterol by other Osh proteins. *A*, *in vitro* sterol transport using recombinant His_6-Osh5, His_6-Osh6, and His_6-Osh7 proteins. The ER and mitochondrial fractions from the *oshΔ osh4-1* strain were incubated in the presence or absence of 5 pmol of His_6-Osh protein at 37 °C for 1 h after preincubation at 37 °C for 30 min. Data are the mean of triplicates of two independent experiments. *Error bars* represent S.E. **, $p < 0.01$; ***, $p < 0.001$ (unpaired *t* test, two-tailed). *B*, binding of Osh proteins to cholesterol *in vitro*. His_6-tagged Osh4 (*black circles*), Osh5 (*dark gray squares*), Osh6 (*medium gray triangles*), and Osh7 (*light gray diamonds*) were incubated with [^{3}H]cholesterol in the presence (*open symbols*) or absence (*closed symbols*) of excess unlabeled cholesterol. $n = 3$. Note that the trend lines of Osh5–Osh7 in the absence of unlabeled cholesterol are similar and that those of Osh4–Osh7 in the presence of unlabeled cholesterol are close to the baseline. *C*, *in vitro* sterol transport using the cytosolic fractions of *OSH* mutant strains. Sterol transport was measured *in vitro* using 200 μg of the cytosol fraction from the *oshΔ osh4-1* strain expressing *OSH1*, *OSH2*, *OSH3*, or *OSH4* at 37 °C for 1 h after preincubation at 37 °C for 30 min. Data are the mean of triplicates of two independent experiments. *Error bars* represent S.E. **, $p < 0.01$; ***, $p < 0.001$ (unpaired *t* test, two-tailed).

Because all Osh proteins mediated sterol transport in our system (Fig. 7, *A* and *C*), one essential function shared by Osh proteins may be intermembrane sterol transport.

Osh4–Osh7 transported 0.09–0.18 ergosterol molecules/Osh protein/min in our *in vitro* sterol transport reaction. When mito-SatA-EGFP was expressed in the *are1Δare2Δ* strain, sterols were esterified at a much higher rate than in the *in vitro* reaction (Fig. 2*B*) (20). Therefore, these *in vitro* transport rates could be slower than those of *in vivo* transport.

The conditions of the *in vitro* sterol transport reaction might not be optimized.

It has been reported that a subset of ORPs transport sterols and PS from the ER to the Golgi and plasma membrane through counterexchange for PI4P. Furthermore, the transport of sterols and PS is coupled with the synthesis and degradation of PI4P (14, 41–43). In our *in vitro* sterol transport reaction, significant sterol transport was observed in the absence of ATP or the presence of EDTA (Fig. 2*C*), suggesting that synthesis of phosphoinositides is not required for *in vitro* sterol transport from the ER to mitochondria, although the presence of phosphoinositides in the mitochondrial membrane needs to be validated. It has been proposed that Osh4 transports sterol against a pre-existing sterol concentration gradient through sterol/PI4P counterexchange using the energy of PI4P hydrolysis (44). Because ergosterol content in the mitochondrial outer membrane is lower than that in the ER in yeast (2), the energy generated by PI4P degradation might not be required for sterol transport from the ER to mitochondria. Further *in vitro* sterol transport analysis using membrane and cytosolic fractions of mutant strains defective in phosphatidylinositol 4-kinases will contribute to elucidating the involvement of PI4P in sterol transport from the ER to mitochondria.

When sterol transport was examined using the ER and mitochondrial fractions from the WT strains (*are1*Δ*are2*Δ), the effect of addition of the cytosolic fraction on sterol transport was less significant (Fig. 2*B*). If Osh4 directly transports sterols to mitochondria, then addition of the cytosolic fraction should increase the transport rate. Therefore, it cannot be denied that Osh4 indirectly affects sterol transport to mitochondria. Osh proteins might mediate sterol transport through forming contact sites between the ER and mitochondria because it was reported that ORDs of Osh proteins simultaneously bind two membranes (23). When the ER and mitochondrial fractions from the *osh*Δ *osh4-1* strain were used, addition of the cytosolic fraction from the WT or *osh*Δ *OSH4* strain significantly facilitated sterol esterification at 37 °C (Fig. 4*D*). In Fig. 3*B*, it was suggested that a fraction of Osh4 localizes to the ER. In addition, it has also been reported that Osh1–Osh3, Osh6, and Osh7 localize to the ER (23, 24). Therefore, sterol transport in the absence of the cytosol could in part be mediated by Osh proteins associated with the ER membranes.

None of the Osh proteins have been shown to be localized to mitochondria. In addition, unambiguous localization of Osh4-FLAG to the mitochondrial membrane was not observed in this study (Fig. 3*B*). Osh proteins may, therefore, be transiently targeted to mitochondria. In mammals, ORP5 and ORP8 are localized to ER-mitochondria contacts in addition to ER-plasma membrane contact sites (45). Because the ORD of ORP5 transports sterol between liposomes *in vitro* (12) and Osh6 and Osh7, which are orthologs of ORP5 and ORP8, transport sterol *in vitro* (23) (Fig. 7*A*), these ORPs could mediate sterol transport from the ER to mitochondria *in vivo*.

Esterification of radiolabeled sterol was observed in the absence of Osh proteins *in vitro* (Figs. 4*D*; 5*B*; and 7, *A* and *B*). Osh-independent sterol transport could be mediated by cytosolic protein(s) associated with membranes or membrane-anchored protein(s). In *S. cerevisiae*, Lam6/Ltc1, a steroidogenic acute regulatory protein-related lipid transfer (StART) domain–containing protein with a transmembrane domain, is localized to the ER-mitochondria contact site, and its cytosolic domain transported sterol between liposomes *in vitro* (46, 47). Thus, Osh-independent sterol transport from the ER to mitochondria could be mediated by a StART domain–containing protein(s). ER-mitochondria contact sites formed by the ER-mitochondria encounter structure complex (ERMES) (48) and the conserved ER membrane protein complex (EMC) (49) have been suggested to be involved in phospholipid transport between the ER and mitochondria in *S. cerevisiae*. A contact site, named the vacuole and mitochondria patch (vCLAMP), between the vacuole and mitochondria (50, 51) was also proposed to serve as a route for phospholipid transport. The role of StART domain–containing proteins and ER-mitochondria contact sites in sterol transport can be determined by analyzing sterol transport using our system.

Sterols play important roles in the structures and functions of various membranes. A system in which sterol acyltransferase is targeted to a membrane of interest in the *are1*Δ*are2*Δ strain and the sterol transport is assessed by determining sterol esterification can be applied to study the transport of sterol synthesized in the ER to other membrane compartments.

Experimental procedures

Strains, media, and plasmids

Strains used in this study are listed in Table 1. *ARE1* and *ARE2* were deleted in the strains W303-1A, CBY924, and CBY926, resulting in the *are1*Δ*are2*Δ, CBY924*are1*Δ*are2*Δ, and CBY926*are1*Δ*are2*Δ strains. The deletion cassette of *ARE1* was constructed by fusion PCR with primers ARE1-Af, ARE1-Af2, ARE1-Ar, ARE1-Bf, ARE1-Br, ARE1-Br2, Nat-U, and Nat-L using the total DNA of W303-1A and pAG25 (52) as templates. The deletion cassette of *ARE2* was similarly constructed with primers ARE2-Af, ARE2-Af2, ARE2-Ar, ARE2-Bf, ARE2-Br, ARE2-Br2, Δare1-U, and Δare1-L using the total DNA of W303-1A and pUG-hph (53) as templates.

Yeast strains were cultivated in YPD (1% yeast extract, 2% peptone, 2% glucose), SD (0.17% yeast nitrogen base without amino acid and ammonium sulfate, 0.5% ammonium sulfate, 2% glucose), and semisynthetic lactate (4.4% lactate, 1.6% NaOH, 0.17% yeast nitrogen base without amino acid and ammonium sulfate, 0.5% ammonium sulfate, 0.3% yeast extract, 0.05% glucose, 0.05% $CaCl_2{\cdot}2H_2O$, 0.05% NaCl, 0.06% $MgCl_2{\cdot}6H_2O$, 0.1% NH_4Cl, 0.1% KH_2PO_4, pH 5.5) media. Methionine was added at a final concentration of 20 mg/liter. *Escherichia coli* was cultivated in LB medium or 2× YT (1.6% bacto Tryptone, 1% yeast extract, 0.5% NaCl) medium.

Plasmids used in this study are listed in Table 2. Primers used for plasmid construction are listed in Table 3. The plasmid YCp33-Osh4-FLAG was constructed as follows. A DNA fragment encoding native promoter and ORF of *OSH4* was amplified with primers BamHI-OSH4 and OSH4-SalI using total DNA of W303-1A as a template, and the amplified fragment was digested with BamHI and SalI and cloned into BamHI-SalI

Table 1
Yeast strains used in this study

Strain	Genotype	Source/Ref.
W303-1A	*MAT*a *ade2-1 ura3-1 his3-11,15 trp1-1 leu2-3,112 can1-100*	ATCC
*are1*Δ*are2*Δ	W303-1A *are1::nat1 are2::hph*	This study
CBY924	*MAT*α *leu2-3,112 ura3-52 his3*Δ*200 lys2-801 trp1*Δ*901 suc2*Δ*9 osh1::kanMX4 osh2::kanMX4 osh3::LYS2 osh4::HIS3 osh5::LEU2 osh6::LEU2 osh7::HIS3* pCB254 (*OSH4 TRP1 CEN*)	26
CBY926	*MAT*α *leu2-3,112 ura3-52 his3*Δ*200 lys2-801 trp1*Δ*901 suc2*Δ*9 osh1::kanMX4 osh2::kanMX4 osh3::LYS2 osh4::HIS3 osh5::LEU2 osh6::LEU2 osh7*Δ*::HIS3* pCB255 (*osh4-1 TRP1 CEN*)	26
CBY924*are1*Δ*are2*Δ	CBY924 *are1::nat1 are2::hph*	This study
CBY926*are1*Δ*are2*Δ	CBY926 *are1::nat1 are2::hph*	This study

Table 2
Plasmids used in this study

Plasmid	Description	Source/Ref.
pAG25	Plasmid carrying nourseothricin resistance gene	52
pUG-hph	Plasmid carrying hygromycin B resistance gene	53
YCplac33	Low-copy vector carrying *URA3*	54
YCplac111	Low-copy vector carrying *LEU2*	54
pMito-SatA	Plasmid to express mito-SatA-EGFP	20
p3×FLAG-Myc-CMV™-26	Plasmid carrying 3 × FLAG	Sigma
YCp33-Osh4-FLAG	YCplac33 carrying *OSH4-FLAG*	This study
YCp33-OSH1	YCplac33 carrying *OSH1*	This study
YCp33-OSH2	YCplac33 carrying *OSH2*	This study
YCp33-OSH3	YCplac33 carrying *OSH3*	This study
pQE30	Expression vector for His_6-tagged protein	Qiagen
pQE30-Osh4	Expression plasmid for His_6-Osh4	This study
pQE30-Osh5	Expression plasmid for His_6-Osh5	This study
pQE30-Osh6	Expression plasmid for His_6-Osh6	This study
pQE30-Osh7	Expression plasmid for His_6-Osh7	This study

sites of YCplac111 (54). A DNA fragment encoding 3×FLAG was amplified with primers SalI-FLAG-f and FLAG-TDH3-r using p3×FLAG-Myc-CMV™-26 (Sigma) as a template. *TDH3* terminator was amplified with primers FLAG-TDH3-f and TDH3-HindIII-r using pMito-SatA (20) as template. A DNA fragment encoding 3×FLAG with *TDH3* terminator was obtained by fusion PCR. The obtained fragment was digested with SalI and HindIII and cloned into SalI-HindIII sites of YCp111-OSH4, resulting in YCp111-Osh4-FLAG. YCp111-Osh4-FLAG was digested with BamHI and HindIII, and a DNA fragment containing the promoter and ORF of *OSH4*, 3×FLAG, and *TDH3* terminator was cloned into BamHI-HindIII sites of YCplac33 (54).

The plasmids YCp33-OSH1, YCp33-OSH2, and YCp33-OSH3 were constructed by the SLiCE (seamless ligation cloning extract) method (55) using DNA fragments amplified with the primers YCp33-Fr and YCp33-rv, OSH1-fr-YCp33 and OSH1-rv-YCp33, OSH2-fr-YCp33 and OSH2-rv-YCp33, and OSH3-fr-YCp33 and OSH3-rv-YCp33 from YCplac33 (54) or the total DNA of W303-1A. The sequences of *OSH* genes were confirmed.

The plasmid pQE30-Osh4 was constructed as follows. The DNA fragment encoding *OSH4* was amplified using total DNA of W303-1A as a template with primers OSH4-U-Bam and OSH4-L-Xho. The amplified fragment was digested with BamHI and SalI and cloned into BamHI-SalI sites of pQE30 (Qiagen), resulting in pQE30-Osh4. Plasmids pQE30-Osh5, pQE30-Osh6, and pQE-Osh7 were constructed similarly as pQE30-Osh4 using primer pairs OSH5-U-Bam and OSH5-L-Xho, OSH6-U-Bam and OSH6-L-Xho, and OSH7-U-Bam and OSH7-L-Xho, respectively.

Preparation of cytosol, ER, and mitochondrial fractions for in vitro sterol transport reaction

The cytosol fractions were prepared from the strains *are1*Δ*are2*Δ, CBY924*are1*Δ*are2*Δ, CBY926*are1*Δ*are2*Δ, CBY924*are1*Δ*are2*Δ containing YCplac33, and CBY926*are1*Δ*are2*Δ containing YCp33-OSH1, YCp33-OSH2, or YCp33-OSH3 as follows. The yeast strains were cultured in 2 (*are1*Δ*are2*Δ and CBY924*are1*Δ*are2*Δ strains) or 4 liters (CBY926*are1*Δ*are2*Δ strain) of YPD medium or 1 liter of SD medium (CBY924*are1*Δ*are2*Δ strain containing YCp33 and CBY926*are1*Δ*are2*Δ strain containing YCp33-OSH1, YCp33-OSH2, or YCp33-OSH3) to an A_{600} of 2.0–2.5. Cells were collected, and spheroplasts were formed according to methods described previously (56) with modifications. Spheroplasts were formed in spheroplast formation buffer (20 mM potassium phosphate, pH 7.2, 1.2 M sorbitol) containing ½ YPD or ½ SD medium. The spheroplasts were suspended in 10 ml of HEPES lysis buffer (25 mM HEPES-KOH, pH 7.4, 100 mM KCl, 10% (w/v) glycerol, 1 mM dithiothreitol (DTT), 1% (v/v) protease inhibitor mixture (Sigma)) and mildly disrupted using a French press (SLM Instruments) at 1,500 p.s.i. Unbroken cells and cell debris were removed by centrifugation at 1,000 × g for 10 min at 4 °C. The supernatant was collected and centrifuged at 13,000 × *g* for 10 min at 4 °C. The supernatant was collected and centrifuged at 100,000 × *g* for 1 h at 4 °C. The supernatant was collected and used as cytosolic fractions.

The ER fractions were prepared from the *are1*Δ*are2*Δ, CBY924*are1*Δ*are2*Δ, and CBY926*are1*Δ*are2*Δ strains as follows. ER fractions were prepared according to the method of Wuestehube and Schekman (57) with modifications. The *are1*Δ*are2*Δ and CBY924*are1*Δ*are2*Δ strains were cultured in 4

Table 3
Primers used in this study
Restriction sites are underlined.

Name	Primer sequence (5′–3′)
ARE1-Af	CCAGAATGAAACTGCACGGCTG
ARE1-Af2	GTCAAAATCTCCCCAGACAG
ARE1-Ar	TCTTGCAATCTGTTTTGGCGCTC
ARE1-Bf	CTGCCACCATACCACGTGTG
ARE1-Br	TCGCCGTCGTTGTCCAACAC
ARE1-Br2	CCTCCACATGGTGCAACGGG
Nat-U	CAAGAGCGCCAAAACAGATTGCAAGAGATCCCCGGGTTAATTAA
Nat-L	CGAGGGACACACGTGGTATGGTGGCAGATATCATCGATGAATTC
ARE2-Af	CGCACTGAGGGTCGCCGAAG
ARE2-Af2	AAAGGTCAACGAAATGCGCC
ARE2-Ar	GTTATTGTTGCTTTTGCTAACG
ARE2-Bf	AAATGTTATTTTCTGGCTCGG
ARE2-Br	ATTGGGAATCCTATTGTGCC
ARE2-Br2	GGGCGGTGGCTTTCATCCTG
Δare1-U	AAGTAAACAGACACATTACGTTAGCAAAAGCAACAATAACAAACACAAC CCAGCTGAAGCTTCGTACGC
Δare1-L	CACTTGGTCCCATGCAGATACCGAGCCAGAAAATAACATTTCCGAGCATA GGCCACTAGTGGATCTG
BamHI-OSH4	CGGGATCCGGACCAGTAACTCATT
OSH4-SalI	ACGCGTCGACCAAAACAATTTCCT
SalI-FLAG-f	ACGCGTCGACGACTACAAAGACCATGACGG
FLAG-TDH3-f	ACAAGGATGACGATGACAAGTTGGTTGAACACGTTGCCAA
FLAG-TDH3-r	TTGGCAACGTGTTCAACCAACTTGTCATCGTCATCCTTGT
TDH3-HindIII-r	CCCAAGCTTTCAATCAATGAATCGAAAAT
YCp33-Fr	TAGAGGATCCCCGGGTAC
YCp33-rv	GCATGCAAGCTTGGCGTA
OSH1-fr-YCp33	TACGCCAAGCTTGCATGCAGATCGACCGCATCTT
OSH1-rv-YCp33	GTACCCGGGGATCCTCTATCGGCTTTGAATCCAT
OSH2-fr-YCp33	TACGCCAAGCTTGCATGCCTTGGCAAACGAATAA
OSH2-rv-YCp33	GTACCCGGGGATCCTCTAACTTTAGCGTCGTAAC
OSH3-fr-YCp33	TACGCCAAGCTTGCATGCTTAGCTGTAATAAGGA
OSH3-rv-YCp33	GTACCCGGGGATCCTCTATCTTCAAAAAACATGG
OSH4-U-Bam	CGGGATCCATGTCTCAATACGCAAGCTC
OSH4-L-Xho	CCGCTCGAGTTACAAAACAATTTCCTTTTC
OSH5-U-Bam	CGGGATCCATGTCTCAACACGCAAGCTC
OSH5-L-Xho	CCGCTCGAGTTATATAGTAATTTCGTTCTC
OSH6-U-Bam	CGGGATCCATGGGCTCCAAAAAACTGAC
OSH6-L-Xho	CCGCTCGAGCTATTGTTTTGCTGGGTTCTG
OSH7-U-Bam	CGGGATCCATGGCTCTCAATAAACTAAAG
OSH7-L-Xho	CCGCTCGAGCTAATTCTTTTGGATTCCATG

liters of YPD medium, and the CBY926*are1*Δ*are2*Δ strain was cultured in 8 liters of YPD medium. Spheroplasts were formed in spheroplast formation buffer containing ½ YPD medium. ER fractions were prepared in two or four batches, respectively, and mixed.

The mitochondrial fractions were prepared from the WT and *are1*Δ*are2*Δ strains containing vector and *are1*Δ*are2*Δ, CBY924*are1*Δ*are2*Δ, and CBY926*are1*Δ*are2*Δ strains containing pMito-SatA (20) according to the method of Zinser and Daum (58) with slight modifications. The yeast strains were precultured in 10 ml of SD medium containing methionine for 1 day and then transferred to 50 ml of semisynthetic lactate medium in 250-ml-scale flasks. After 1-day cultivation, cells were transferred to 1 liter of semisynthetic lactate medium in 5-liter-scale flasks and incubated until A_{600} reached 2.0–2.5. Spheroplasts were formed in spheroplast formation buffer containing ½ semisynthetic lactate medium. The spheroplasts were suspended in 20 ml of MES lysis buffer (20 mM MES-KOH, pH 6.0, 0.6 M sorbitol, 1 mM DTT, 1% (v/v) protease inhibitor mixture) and mildly disrupted using a French press at 1,500 p.s.i. Unbroken cells and cell debris were removed by centrifugation at 1,500 × *g* for 5 min at 4 °C, and the supernatant was collected. The pellets were resuspended in 10 ml of MES lysis buffer and centrifuged at 1,500 × *g* for 5 min at 4 °C, and the supernatant was collected. This washing process was repeated. The supernatants were mixed and used as the whole-cell extracts. The whole-cell extracts were centrifuged at 13,000 × *g* for 10 min at 4 °C, and the pellets were resuspended in 2 ml of MES lysis buffer (P13 fraction). Two milliliters of the P13 fraction was loaded on 11 ml of sucrose step gradient containing 5.5 ml of 30% (w/v) sucrose in MES lysis buffer and 5.5 ml of 60% (w/v) sucrose in MES lysis buffer and centrifuged in the swing rotor at 28,000 rpm for 3 h at 4 °C. The membranes at the 30%/60% interface were collected, washed once with MES lysis buffer, and resuspended in buffer containing 25 mM HEPES, pH 7.5, 100 mM KCl, 10% (w/v) glycerol, 1 mM DTT, 1% (v/v) protease inhibitor mixture. The WT and *are1*Δ*are2*Δ strains containing vector and the *are1*Δ*are2*Δ strain containing pMito-SatA were cultured in 1 liter of semisynthetic lactate medium for steryl ester detection. The *are1*Δ*are2*Δ and CBY924*are1*Δ*are2*Δ strains were cultured in 4 liters of semisynthetic lactate medium, and the CBY926*are1*Δ*are2*Δ strain was cultured in 12 liters of semisynthetic lactate medium in total. Mitochondrial fractions were prepared in four or six batches, respectively, and mixed. The purity of ER and mitochondrial fractions was analyzed by immunoblotting using anti-Kar2 (59) and anti-Cox2 (Invitrogen) antibodies as described previously (20).

Protein purification

E. coli MV1990 (Toyobo) strain harboring plasmid pQE30-Osh4, pQE30-Osh5, pQE30-Osh6, or pQE30-Osh7 was culti-

vated to an A_{600} 0.4–0.5 in 500 ml of LB medium or to an A_{600} of 0.7 in 1,000 ml of 2× YT medium at 25 °C. Following 4–6 h of incubation with 0.1 mM isopropyl β-D-thiogalactopyranoside, cells were collected and broken using a French press in breaking buffer (25 mM HEPES-KOH, pH 7.4, 100 mM KCl (for His_6-Osh4) or 400 mM KCl (for His_6-Osh5, Osh6, and Osh7), 10% (w/v) glycerol, 1 mM DTT, 0.5% (v/v) protease inhibitor mixture) for use in purification of histidine-tagged proteins (Sigma). Cell lysate was centrifuged at 18,000 × *g* for 30 min at 4 °C. The supernatant was incubated overnight at 4 °C with Profinity immobilized metal affinity chromatography nickel-charged resin (Bio-Rad) equilibrated with breaking buffer. The resin was extensively washed first with breaking buffer containing 1% (v/v) Triton X-100, then with breaking buffer without Triton X-100, and finally with breaking buffer containing 20 mM imidazole. Protein was eluted from the resin with breaking buffer containing 500 mM imidazole. The buffer was exchanged using a NAP-5 column (GE Healthcare) to buffer A (25 mM HEPES-KOH, pH 7.4, 100 mM KCl, 10% (w/v) glycerol, 1 mM DTT).

Sterol transport assay in vitro and in vitro

Sterols were synthesized *in vitro* as described (22) with slight modification as follows. The reaction mixture (50 μl) containing the ER fractions (100 μg of protein), cytosolic fractions (200 μg), 3 mM reduced GSH, 3 mM glucose 6-phosphate, 1 unit of glucose-6-phosphate dehydrogenase, 5 mM ATP, 1 mM NADPH, 1 mM NADP, 1 mM NAD, 2 μCi of L-[*methyl*-^{3}H]methionine (PerkinElmer Life Sciences), 25 mM HEPES (pH 7.4), 100 mM KCl, 10% glycerol, 5 mM $MgCl_2$, and 2 mM $MnCl_2$ was incubated at 30 or 25 °C. After 1-h incubation, the reaction mixture was centrifuged at 27,000 × *g* for 11 min at 4 °C. The pellets were suspended in buffer containing 25 mM HEPES-KOH, pH 7.4, 100 mM KCl, 10% (w/v) glycerol, 1 mM DTT, and 1% (v/v) protease inhibitor mixture and used as ER fractions for the sterol transport assay. The sterol transport assay was performed as follows. The reaction mixture (50 μl) containing the ER fraction obtained as described above and the mitochondrial fractions (150 μg of protein) in the presence or absence of the cytosolic fractions (200 μg of protein) or purified proteins was incubated at 30 or 37 °C. In the reaction with preincubation, the ER and cytosolic fractions or Osh proteins and the mitochondrial fraction were separately preincubated at 25 or 37 °C for 30 min after which these fractions and proteins were mixed and incubated at the same temperature for 1 h. The reaction was stopped by addition of chloroform/methanol (1:2, v/v). Lipids were extracted by the method of Bligh and Dyer (60), dissolved in chloroform/methanol (2:1, v/v), and separated by thin layer chromatography (TLC) on Silica Gel 60 (Merck, 5721) with hexane/diethyl ether/acetic acid (80:20:1, v/v/v) as a developing solvent. After spraying with sulfuric acid/acetic acetate (1:1, v/v), plates were heated at 90 °C for 10 min. Sterols and steryl esters were scraped off the TLC plate, and their radioactivities were determined by a liquid scintillation counter (Aloka) using Clear-sol I (Nacalai Tesque).

To examine the integrity of the mitochondrial membrane during the *in vitro* sterol transport reaction, the reaction mixture (50 μl) containing the ER fraction (100 μg of protein) from the *are1*Δ*are2*Δ strain, the mitochondrial fraction from the *are1*Δ*are2*Δ strain expressing mito-SatA-EGFP (150 μg of protein), 25 mM HEPES-KOH, pH 7.4, 100 mM KCl, and 10% (w/v) glycerol was incubated at 30 °C for 1 h. After the incubation, samples were treated with 1 μg/ml proteinase K (Wako) in the absence or presence of 0.2% Triton X-100 at 4 °C for 30 min. Cox2 was detected by Western blotting using antibody against Cox2.

The *in vivo* sterol transport assay was performed as described previously (20) with modifications as follows. The *osh*Δ *OSH4* and *osh*Δ *osh4-1* strains containing pMito-SatA (20) were cultivated at 25 °C overnight in SD medium containing methionine. Cells were harvested and washed twice in SD medium. Cells were resuspended in SD medium at 5 A_{600}/ml and incubated at 25 °C for 1 h and then at 25 or 37 °C for 30 min. L-[*methyl*-^{3}H]Methionine was added at a final concentration of 2 μCi/ml, and cells were further incubated at 25 or 37 °C for 5 min. Lipids were extracted, and their radioactivities were determined.

Analysis of Osh4-FLAG distribution

The W303−1A strain containing YCp111-Osh4-FLAG was cultured in 2 liters of SD medium until A_{600} reached 1.5–2.0. Cells were collected, and spheroplasts were prepared. The spheroplasts were suspended in 20 ml of MES lysis buffer and mildly disrupted using a French press at 1,500 p.s.i. Unbroken cells and cell debris were removed by centrifugation at 1,000 × *g* for 10 min at 4 °C, and the supernatant was collected. The pellet was suspended in 10 ml of MES lysis buffer and centrifuged at 1,000 × *g* for 10 min at 4 °C, and the supernatant was collected. The supernatant was mixed and used as whole-cell extracts. An aliquot of the whole-cell extracts was used to prepare fractions of mitochondria, and another aliquot of the whole-cell extracts was used to prepare ER and cytosolic fractions as described above. The recovery of the ER and mitochondria in obtained fractions was confirmed as described previously (20). The recovery of Osh4-FLAG and Pgk1 was analyzed by Western blot analysis using anti-FLAG M2 (Sigma) and anti-Pgk1 (Abcam) antibodies. Images were obtained using a LAS-500 (Fujifilm), and band intensity was quantitated with Image Gauge 3.4 (Fujifilm).

Quantification of ergosterol in fractions

The CBY924 and CBY926 strains were cultured in 800 ml of YPD medium to an A_{600} of 2.0 at 25 °C after which cells were incubated at 25 or 37 °C for 80 min. Spheroplasts were formed in 10 ml of spheroplast formation buffer containing ½ YPD medium at 25 or 37 °C, respectively. The spheroplasts were suspended in MES lysis buffer and mildly disrupted using a French press. Unbroken cells and cell debris were removed by centrifugation at 1,500 × *g* for 5 min at 4 °C, and the supernatant was collected. The pellets were resuspended in 14 ml of MES lysis buffer and centrifuged at 1,500 × *g* for 5 min at 4 °C, and the supernatant was collected. The supernatants were mixed and used as whole-cell extracts. Small aliquots of the whole-cell extracts were separated for the quantification of ergosterol and phospholipids. One-third of the whole-cell extracts was used for the preparation of the ER fractions, and two-thirds of the whole-cell extracts was used for the preparation of the mitochondrial fractions as described above. Lipids in the whole-cell

extracts, ER fraction, and mitochondrial fraction were extracted as described above. Cholesterol was added to each sample for use as an internal standard. Extracted lipids were dried under nitrogen, dissolved in ethyl acetate, and analyzed by GC-MS suing QP2010 SE (Shimadzu) with a DB5 capillary column (30 m × 0.25 mm; J & W Scientific). Samples were injected at a 280 °C injection temperature with helium as a carrier gas. The following temperature program was used: 1 min at 120 °C, 75 °C/min to 270 °C, 3 °C/min to 300 °C, and 3-min hold at 300 °C. Total phospholipid contents of the whole-cell extracts, ER fraction, and mitochondrial fraction were determined by phosphorus assay according to the method of Bartlett (61). The ergosterol content in the ER fraction of the CBY926*are1*Δ*are2*Δ strain used for the *in vitro* sterol transport assay was measured by GC-MS as described above.

Sterol acyltransferase activity assay

The sterol acyltransferase activity assay was performed as described (62) with slight modifications. Each reaction contained the mitochondrial fractions (150 μg) from the *osh*Δ *OSH4* or *osh*Δ *osh4-1* strain, 25 mM HEPSE-KOH, pH 7.5, 100 mM KCl, 1 mM DTT, and 0.1 μCi of [4-^{14}C]cholesterol (American Radiolabeled Chemicals Inc.) in a total volume of 50 μl. The reaction was performed at 37 °C for 1 h and stopped by the addition of chloroform/methanol (1:2, v/v). Sterols and steryl esters were extracted and separated by TLC. Their radioactivities were measured as described above.

Sterol binding assay

[1,2-^{3}H]Cholesterol (PerkinElmer Life Sciences) binding by Osh proteins was performed as described (63) with slight modifications as follows. His$_6$-tagged Osh proteins (10 pmol) were incubated in 50 μl of binding buffer (25 mM HEPES-KOH, pH 7.4, 100 mM KCl, 0.05% Triton X-100) containing radioactive cholesterol in the presence or absence of a 40-fold excess of unlabeled cholesterol. After incubation at 25 °C for 1 h, 10 μl of nickel-charged resin (Bio-Rad) was added and incubated for 15 min at 25 °C. The resin was pelleted by centrifuge at 15,000 rpm for 1 min. After three washes with wash buffer (25 mM HEPES-KOH, pH 7.4, 100 mM KCl), the proteins were eluted from the resin with 710 μl of elution buffer (25 mM HEPES-KOH, pH 7.4, 100 mM KCl, 150 mM imidazole). After centrifugation at 15,000 rpm for 10 min, radioactivities in the supernatants were determined as described above. Binding curves were plotted, and K_d and B_{max} were determined using GraphPad Prism software.

Author contributions—S. T., A. O., and R. F. conceptualization; S. T., A. O., H. H., and R. F. data curation; S. T., A. O., H. H., and R. F. formal analysis; S. T. and R. F. funding acquisition; S. T. and R. F. investigation; S. T. writing-original draft; A. O., H. H., and R. F. resources; A. O., H. H., and R. F. project administration; A. O., H. H., and R. F. writing-review and editing; H. H. and R. F. supervision; R. F. methodology.

Acknowledgments—We thank Dr. C. T. Beh for strains CBY924 and CBY926 and Dr. Masao Tokunaga for anti-Kar2 antibody. This work was done using the facilities of the Biotechnology Research Center of the University of Tokyo.

References

1. Maxfield, F. R., and Menon, A. K. (2006) Intracellular sterol transport and distribution. *Curr. Opin. Cell Biol.* **18,** 379–385 CrossRef Medline
2. Zinser, E., Sperka-Gottlieb, C. D., Fasch, E. V., Kohlwein, S. D., Paltauf, F., and Daum, G. (1991) Phospholipid synthesis and lipid composition of subcellular membranes in the unicellular eukaryote *Saccharomyces cerevisiae*. *J. Bacteriol.* **173,** 2026–2034 CrossRef Medline
3. Mesmin, B., Antonny, B., and Drin, G. (2013) Insights into the mechanisms of sterol transport between organelles. *Cell. Mol. Life Sci.* **70,** 3405–3421 CrossRef Medline
4. Urbani, L., and Simoni, R. D. (1990) Cholesterol and vesicular stomatitis virus G protein take separate routes from the endoplasmic reticulum to the plasma membrane. *J. Biol. Chem.* **265,** 1919–1923 Medline
5. Heino, S., Lusa, S., Somerharju, P., Ehnholm, C., Olkkonen, V. M., and Ikonen, E. (2000) Dissecting the role of the Golgi complex and lipid rafts in biosynthetic transport of cholesterol to the cell surface. *Proc. Natl. Acad. Sci. U.S.A.* **97,** 8375–8380 CrossRef Medline
6. Li, Y., and Prinz, W. A. (2004) ATP-binding cassette (ABC) transporters mediate nonvesicular, raft-modulated sterol movement from the plasma membrane to the endoplasmic reticulum. *J. Biol. Chem.* **279,** 45226–45234 CrossRef Medline
7. Baumann, N. A., Sullivan, D. P., Ohvo-Rekilä, H., Simonot, C., Pottekat, A., Klaassen, Z., Beh, C. T., and Menon, A. K. (2005) Transport of newly synthesized sterol to the sterol-enriched plasma membrane occurs via nonvesicular equilibration. *Biochemistry* **44,** 5816–5826 CrossRef Medline
8. Holthuis, J. C., and Menon, A. K. (2014) Lipid landscapes and pipelines in membrane homeostasis. *Nature* **510,** 48–57 CrossRef Medline
9. Kentala, H., Weber-Boyvat, M., and Olkkonen, V. M. (2016) OSBP-related protein family: mediators of lipid transport and signaling at membrane contact sites. *Int. Rev. Cell Mol. Biol.* **321,** 299–340 CrossRef Medline
10. Raychaudhuri, S., Im, Y. J., Hurley, J. H., and Prinz, W. A. (2006) Nonvesicular sterol movement from plasma membrane to ER requires oxysterol-binding protein-related proteins and phosphoinositides. *J. Cell Biol.* **173,** 107–119 CrossRef Medline
11. Ngo, M., and Ridgway, N. D. (2009) Oxysterol binding protein-related protein 9 (ORP9) is a cholesterol transfer protein that regulates Golgi structure and function. *Mol. Biol. Cell* **20,** 1388–1399 CrossRef Medline
12. Du, X., Kumar, J., Ferguson, C., Schulz, T. A., Ong, Y. S., Hong, W., Prinz, W. A., Parton, R. G., Brown, A. J., and Yang, H. (2011) A role for oxysterol-binding protein-related protein 5 in endosomal cholesterol trafficking. *J. Cell Biol.* **192,** 121–135 CrossRef Medline
13. Maeda, K., Anand, K., Chiapparino, A., Kumar, A., Poletto, M., Kaksonen, M., and Gavin, A. C. (2013) Interactome map uncovers phosphatidylserine transport by oxysterol-binding proteins. *Nature* **501,** 257–261 CrossRef Medline
14. Chung, J., Torta, F., Masai, K., Lucast, L., Czapla, H., Tanner, L. B., Narayanaswamy, P., Wenk, M. R., Nakatsu, F., and De Camilli, P. (2015) Intracellular transport. PI4P/phosphatidylserine countertransport at ORP5- and ORP8-mediated ER-plasma membrane contacts. *Science* **349,** 428–432 CrossRef Medline
15. Beh, C. T., Cool, L., Phillips, J., and Rine, J. (2001) Overlapping functions of the yeast oxysterol-binding protein homologues. *Genetics* **157,** 1117–1140 Medline
16. Horvath, S. E., and Daum, G. (2013) Lipids of mitochondria. *Prog. Lipid Res.* **52,** 590–614 CrossRef Medline
17. Martin, L. A., Kennedy, B. E., and Karten, B. (2016) Mitochondrial cholesterol: mechanisms of import and effects on mitochondrial function. *J. Bioenerg. Biomembr.* **48,** 137–151 CrossRef Medline
18. Altmann, K., and Westermann, B. (2005) Role of essential genes in mitochondrial morphogenesis in *Saccharomyces cerevisiae*. *Mol. Biol. Cell* **16,** 5410–5417 CrossRef Medline
19. Soffientini, U., and Graham, A. (2016) Intracellular cholesterol transport proteins: roles in health and disease. *Clin. Sci.* **130,** 1843–1859 CrossRef Medline
20. Tian, S., Ohta, A., Horiuchi, H., and Fukuda, R. (2015) Evaluation of sterol transport from the endoplasmic reticulum to mitochondria using mito-

chondrially targeted bacterial sterol acyltransferase in *Saccharomyces cerevisiae*. *Biosci. Biotechnol. Biochem.* **79,** 1608–1614 CrossRef Medline
21. Vipond, R., Bricknell, I. R., Durant, E., Bowden, T. J., Ellis, A. E., Smith, M., and MacIntyre, S. (1998) Defined deletion mutants demonstrate that the major secreted toxins are not essential for the virulence of *Aeromonas salmonicida*. *Infect. Immun.* **66,** 1990–1998 Medline
22. Venkateswarlu, K., Lamb, D. C., Kelly, D. E., Manning, N. J., and Kelly, S. L. (1998) The N-terminal membrane domain of yeast NADPH-cytochrome P450 (CYP) oxidoreductase is not required for catalytic activity in sterol biosynthesis or in reconstitution of CYP activity. *J. Biol. Chem.* **273,** 4492–4496 CrossRef Medline
23. Schulz, T. A., Choi, M. G., Raychaudhuri, S., Mears, J. A., Ghirlando, R., Hinshaw, J. E., and Prinz, W. A. (2009) Lipid-regulated sterol transfer between closely apposed membranes by oxysterol-binding protein homologues. *J. Cell Biol.* **187,** 889–903 CrossRef Medline
24. Levine, T. P., and Munro, S. (2001) Dual targeting of Osh1p, a yeast homologue of oxysterol-binding protein, to both the Golgi and the nucleus-vacuole junction. *Mol. Biol. Cell* **12,** 1633–1644 CrossRef Medline
25. Fairn, G. D., Curwin, A. J., Stefan, C. J., and McMaster, C. R. (2007) The oxysterol binding protein Kes1p regulates Golgi apparatus phosphatidylinositol-4-phosphate function. *Proc. Natl. Acad. Sci. U.S.A.* **104,** 15352–15357 CrossRef Medline
26. Beh, C. T., and Rine, J. (2004) A role for yeast oxysterol-binding protein homologs in endocytosis and in the maintenance of intracellular sterol-lipid distribution. *J. Cell Sci.* **117,** 2983–2996 CrossRef Medline
27. Kulak, N. A., Pichler, G., Paron, I., Nagaraj, N., and Mann, M. (2014) Minimal, encapsulated proteomic-sample processing applied to copy-number estimation in eukaryotic cells. *Nat. Methods* **11,** 319–324 CrossRef Medline
28. Leventis, R., and Silvius, J. R. (2001) Use of cyclodextrins to monitor transbilayer movement and differential lipid affinities of cholesterol. *Biophys. J.* **81,** 2257–2267 CrossRef Medline
29. Tong, J., Yang, H., Yang, H., Eom, S. H., and Im, Y. J. (2013) Structure of Osh3 reveals a conserved mode of phosphoinositide binding in oxysterol-binding proteins. *Structure* **21,** 1203–1213 CrossRef Medline
30. Suchanek, M., Hynynen, R., Wohlfahrt, G., Lehto, M., Johansson, M., Saarinen, H., Radzikowska, A., Thiele, C., and Olkkonen, V. M. (2007) The mammalian oxysterol-binding protein-related proteins (ORPs) bind 25-hydroxycholesterol in an evolutionarily conserved pocket. *Biochem. J.* **405,** 473–480 CrossRef Medline
31. Alfaro, G., Johansen, J., Dighe, S. A., Duamel, G., Kozminski, K. G., and Beh, C. T. (2011) The sterol-binding protein Kes1/Osh4p is a regulator of polarized exocytosis. *Traffic* **12,** 1521–1536 CrossRef Medline
32. Georgiev, A. G., Sullivan, D. P., Kersting, M. C., Dittman, J. S., Beh, C. T., and Menon, A. K. (2011) Osh proteins regulate membrane sterol organization but are not required for sterol movement between the ER and PM. *Traffic* **12,** 1341–1355 CrossRef Medline
33. Perry, R. J., and Ridgway, N. D. (2006) Oxysterol-binding protein and vesicle-associated membrane protein-associated protein are required for sterol-dependent activation of the ceramide transport protein. *Mol. Biol. Cell* **17,** 2604–2616 CrossRef Medline
34. Kajiwara, K., Ikeda, A., Aguilera-Romero, A., Castillon, G. A., Kagiwada, S., Hanada, K., Riezman, H., Muñiz, M., and Funato, K. (2014) Osh proteins regulate COPII-mediated vesicular transport of ceramide from the endoplasmic reticulum in budding yeast. *J. Cell Sci.* **127,** 376–387 CrossRef Medline
35. Stefan, C. J., Manford, A. G., Baird, D., Yamada-Hanff, J., Mao, Y., and Emr, S. D. (2011) Osh proteins regulate phosphoinositide metabolism at ER-plasma membrane contact sites. *Cell* **144,** 389–401 CrossRef Medline
36. Mousley, C. J., Yuan, P., Gaur, N. A., Trettin, K. D., Nile, A. H., Deminoff, S. J., Dewar, B. J., Wolpert, M., Macdonald, J. M., Herman, P. K., Hinnebusch, A. G., and Bankaitis, V. A. (2012) A sterol-binding protein integrates endosomal lipid metabolism with TOR signaling and nitrogen sensing. *Cell* **148,** 702–715 CrossRef Medline
37. Tavassoli, S., Chao, J. T., Young, B. P., Cox, R. C., Prinz, W. A., de Kroon, A. I., and Loewen, C. J. (2013) Plasma membrane–endoplasmic reticulum contact sites regulate phosphatidylcholine synthesis. *EMBO Rep.* **14,** 434–440 CrossRef Medline
38. Wang, P. Y., Weng, J., and Anderson, R. G. (2005) OSBP is a cholesterol-regulated scaffolding protein in control of ERK 1/2 activation. *Science* **307,** 1472–1476 CrossRef Medline
39. Romeo, G. R., and Kazlauskas, A. (2008) Oxysterol and diabetes activate STAT3 and control endothelial expression of profilin-1 via OSBP1. *J. Biol. Chem.* **283,** 9595–9605 CrossRef Medline
40. Bowden, K., and Ridgway, N. D. (2008) OSBP negatively regulates ABCA1 protein stability. *J. Biol. Chem.* **283,** 18210–18217 CrossRef Medline
41. de Saint-Jean, M., Delfosse, V., Douguet, D., Chicanne, G., Payrastre, B., Bourguet, W., Antonny, B., and Drin, G. (2011) Osh4p exchanges sterols for phosphatidylinositol 4-phosphate between lipid bilayers. *J. Cell Biol.* **195,** 965–978 CrossRef Medline
42. Mesmin, B., Bigay, J., Moser von Filseck, J., Lacas-Gervais, S., Drin, G., and Antonny, B. (2013) A four-step cycle driven by PI(4)P hydrolysis directs sterol/PI(4)P exchange by the ER-Golgi tether OSBP. *Cell* **155,** 830–843 CrossRef Medline
43. Moser von Filseck, J., Čopič, Delfosse, V., Vanni, S., Jackson, C. L., Bourguet, W., and Drin, G. (2015) Intracellular transport. Phosphatidylserine transport by ORP/Osh proteins is driven by phosphatidylinositol 4-phosphate. *Science* **349,** 432–436 CrossRef Medline
44. Moser von Filseck, J., Vanni, S., Mesmin, B., Antonny, B., and Drin, G. (2015) A phosphatidylinositol-4-phosphate powered exchange mechanism to create a lipid gradient between membranes. *Nat. Commun.* **6,** 6671 CrossRef Medline
45. Galmes, R., Houcine, A., van Vliet, A. R., Agostinis, P., Jackson, C. L., and Giordano, F. (2016) ORP5/ORP8 localize to endoplasmic reticulum-mitochondria contacts and are involved in mitochondrial function. *EMBO Rep.* **17,** 800–810 CrossRef Medline
46. Murley, A., Sarsam, R. D., Toulmay, A., Yamada, J., Prinz, W. A., and Nunnari, J. (2015) Ltc1 is an ER-localized sterol transporter and a component of ER-mitochondria and ER-vacuole contacts. *J. Cell Biol.* **209,** 539–548 CrossRef Medline
47. Gatta, A. T., Wong, L. H., Sere, Y. Y., Calderón-Noreña, D. M., Cockcroft, S., Menon, A. K., and Levine, T. P. (2015) A new family of StART domain proteins at membrane contact sites has a role in ER-PM sterol transport. *Elife* **4,** e07253 CrossRef Medline
48. Kornmann, B., Currie, E., Collins, S. R., Schuldiner, M., Nunnari, J., Weissman, J. S., and Walter, P. (2009) An ER-mitochondria tethering complex revealed by a synthetic biology screen. *Science* **325,** 477–481 CrossRef Medline
49. Lahiri, S., Chao, J. T., Tavassoli, S., Wong, A. K., Choudhary, V., Young, B. P., Loewen, C. J., and Prinz, W. A. (2014) A conserved endoplasmic reticulum membrane protein complex (EMC) facilitates phospholipid transfer from the ER to mitochondria. *PLoS Biol.* **12,** e1001969 CrossRef Medline
50. Elbaz-Alon, Y., Rosenfeld-Gur, E., Shinder, V., Futerman, A. H., Geiger, T., and Schuldiner, M. (2014) A dynamic interface between vacuoles and mitochondria in yeast. *Dev. Cell* **30,** 95–102 CrossRef Medline
51. Hönscher, C., Mari, M., Auffarth, K., Bohnert, M., Griffith, J., Geerts, W., van der Laan, M., Cabrera, M., Reggiori, F., and Ungermann, C. (2014) Cellular metabolism regulates contact sites between vacuoles and mitochondria. *Dev. Cell* **30,** 86–94 CrossRef Medline
52. Goldstein, A. L., and McCusker, J. H. (1999) Three new dominant drug resistance cassettes for gene disruption in *Saccharomyces cerevisiae*. *Yeast* **15,** 1541–1553 CrossRef Medline
53. Deng, L., Fukuda, R., Kakihara, T., Narita, K., and Ohta, A. (2010) Incorporation and remodeling of phosphatidylethanolamine containing short acyl residues in yeast. *Biochim. Biophys. Acta* **1801,** 635–645 CrossRef Medline
54. Gietz, R. D., and Sugino, A. (1988) New yeast-*Escherichia coli* shuttle vectors constructed with *in vitro* mutagenized yeast genes lacking six-base pair restriction sites. *Gene* **74,** 527–534 CrossRef Medline
55. Motohashi, K. (2015) A simple and efficient seamless DNA cloning method using SLiCE from *Escherichia coli* laboratory strains and its application to SLiP site-directed mutagenesis. *BMC Biotechnol.* **15,** 47 CrossRef Medline
56. Kobayashi, S., Mizuike, A., Horiuchi, H., Fukuda, R., and Ohta, A. (2014) Mitochondrially-targeted bacterial phosphatidylethanolamine methyltransferase sustained phosphatidylcholine synthesis of a *Saccharomyces cerevisiae* Δ*pem1* Δ*pem2* double mutant without exogenous choline supply. *Biochim. Biophys. Acta* **1841,** 1264–1271 CrossRef Medline

57. Wuestehube, L. J., and Schekman, R. W. (1992) Reconstitution of transport from endoplasmic reticulum to Golgi complex using endoplasmic reticulum-enriched membrane fraction from yeast. *Methods Enzymol.* **219,** 124–136 CrossRef Medline
58. Zinser, E., and Daum, G. (1995) Isolation and biochemical characterization of organelles from the yeast, *Saccharomyces cerevisiae*. *Yeast* **11,** 493–536 CrossRef Medline
59. Tokunaga, M., Kawamura, A., and Kohno, K. (1992) Purification and characterization of BiP/Kar2 protein from *Saccharomyces cerevisiae*. *J. Biol. Chem.* **267,** 17553–17559 Medline
60. Bligh, E. G., and Dyer, W. J. (1959) A rapid method of total lipid extraction and purification. *Can. J. Biochem. Physiol.* **37,** 911–917 CrossRef Medline
61. Bartlett, G. R. (1959) Phosphorus assay in column chromatography. *J. Biol. Chem.* **234,** 466–468 Medline
62. Buckley, J. T., Halasa, L. N., and MacIntyre, S. (1982) Purification and partial characterization of a bacterial phospholipid: cholesterol acyltransferase. *J. Biol. Chem.* **257,** 3320–3325 Medline
63. Im, Y. J., Raychaudhuri, S., Prinz, W. A., and Hurley, J. H. (2005) Structural mechanism for sterol sensing and transport by OSBP-related proteins. *Nature* **437,** 154–158 CrossRef Medline